

Geometric Calibration of Acoustic Camera Star48 Array

Christian MANTHE, Andy MEYER, Frank GIELSDORF, Germany

Key words: calibration, acoustic camera, quaternion rotation

SUMMARY

Acoustic emission monitoring is getting increasingly important with engineering product design. An acoustic camera was recently developed as a new measuring device and constitutes a strong innovation made for localizing noise emissions. This article describes the operation of the acoustic camera with special focus on the geometric calibration with engineering surveying methods.

For the acoustic camera a digital camera is used to acquire an image of the noise-emitting object. At the same time an exactly computed array of microphones acquires and records the sound waves emitted by the object. Dedicated software then calculates a sound map and combines the acoustical and the optical images of the noise source.

A precise determination of the relative spatial position of the microphones of better than $\pm 0.5\text{mm}$ is crucial to the angular precision of the acoustic camera and thus is important for the absolute position of the noise emission. In order to achieve the required geometric precision the method of intersection combined with quaternion-rotation is applied to the specific geometric design of microphone array calibration.

Geometric Calibration of Acoustic Camera Star48 Array

Christian MANTHE, Andy MEYER, Frank GIELSDORF, Germany

1. FUNCTIONALITY OF THE ACOUSTIC CAMERA

The use of microphone arrays and multichannel data recorders in connection with software for a fast visualization results an Acoustic Camera. Such a device has become popular for the localization of sound sources of machinery and equipment of any kind. An overlay of an optical photo gives the user a fast overview of the dominant noise sources emitted by the device under test (Jaeckel, 2006).

The underlying common principle of those systems in the far field approach is the delay-and-sum beamforming method (Figure 1). That technique use special time delay sets for the incoming signals to focus the microphone array on a spatial location. The correct delay set results in a coherent overlay by adding up all microphone signals. With that special time delay the region emitting the strongest sound pressure can be found.

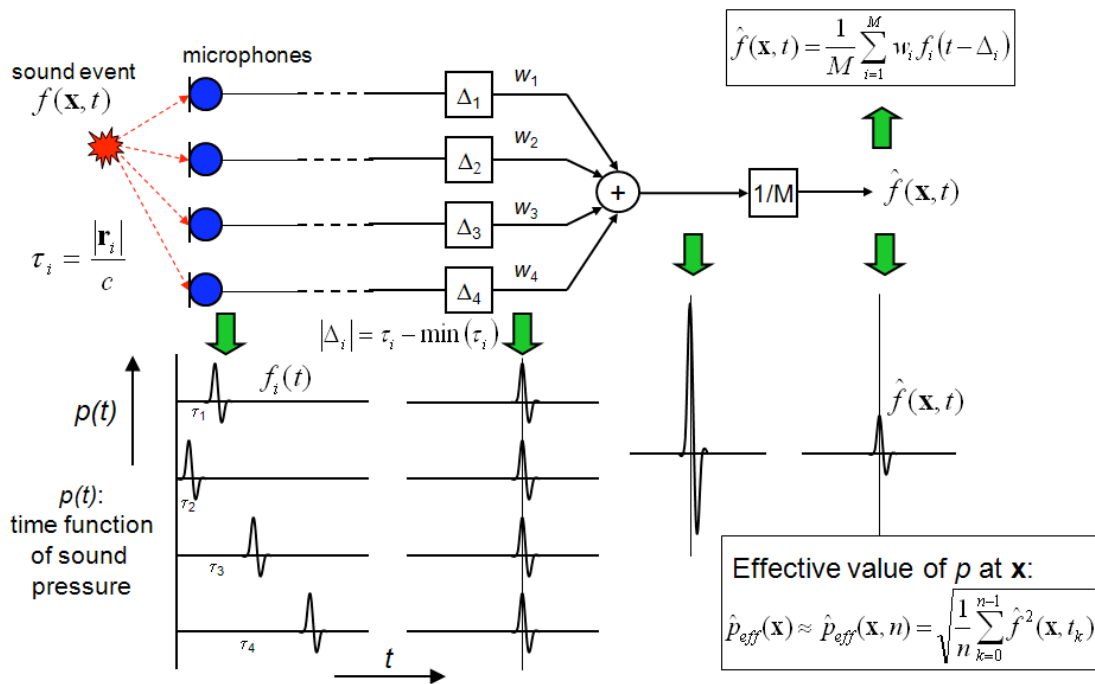


Figure 1 overview of the delay and sum beamforming method (©GfaI)

Applying that beamforming technique for each pixel in a measurement plane (Figure 2) generates a sound pressure image.

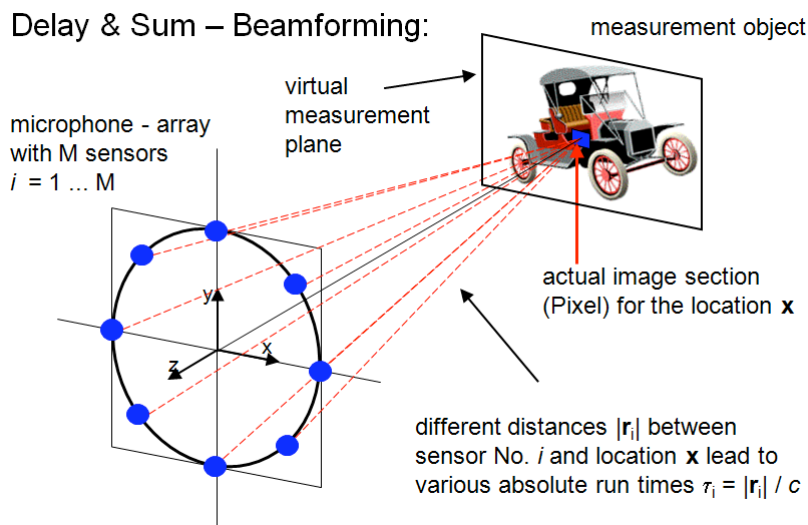


Figure 2 delay-sum beamforming and the acoustic camera (©GfaI)

2. REALIZATION OF THE STAR48 ARRAY

The frequency range of such devices is correlated with the size of the acoustic camera. The star array (

Figure 3) is developed to realize a portable system with a size about 3m in diameter. That gives the opportunity to detect also the deeper frequencies, interesting for large objects. The star array has three hinged lightly inclined microphone arms and a digital camera in the center. To get accurate microphone positions the microphone holes (about 1mm diameter) on each arm are drilled with a CNC-Milling machine (precision about $\pm 0.1\text{mm}$). Each microphone is connected with a recorder witch support very high scan-rates on 48 channels to record the sound.

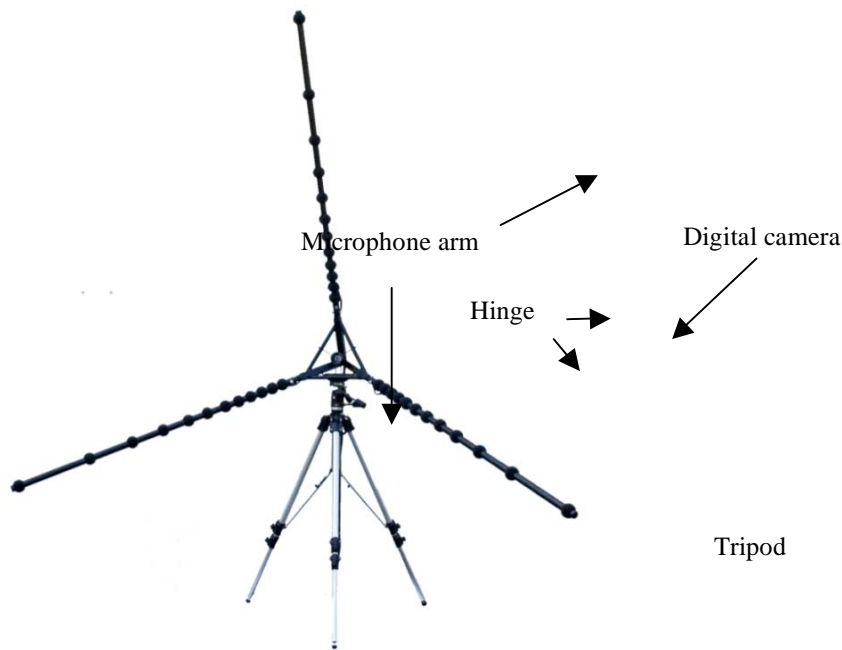


Figure 3 star array

3. GEOMETRIC CALLIBRATION

Since the mechanical construction is a subject to inexactness the as-built microphone positions must be calibrated. The real microphone coordinates deviate from the theoretical coordinates. The developed calibration software is applied immediately after delivery in order to provide the exact microphone positions to the customer. It runs right in time and place, not requiring any post processing in the office.

3.1 Spatial geometric localization of the microphones

The manufactured microphones have to be precisely coordinated in order to obtain a better time delay for each microphone with respect to each acoustic image pixel. The calibration will improve the angular resolution of the acoustic camera (figure 5).

Therefore different geometric measurement methods are possible. A close range photogrammetric approach would require a great number of high resolution pictures and hence was considered as being too expensive. A coordinate measuring machine is expensive and has to touch the sensible microphone array.

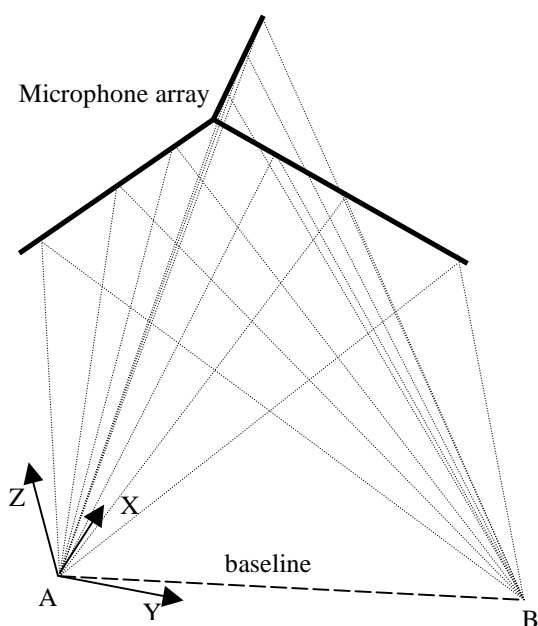


Figure 3 measurement configuration

Measurement device

A total station Leica TCA 2003 ($\pm 0.3\text{mgon}$, $\pm 1\text{mm}$ at a 68% level of significance) is used for the angle and distance observation. The pre-measurement analysis showed that a survey procedure with two standpoints (A and B) and directions being observed two times in two faces lead to a sufficient result.

3.2 Estimation of the microphone coordinates

The general outline of the accomplished algorithm is the following: First the observations are adjusted in a local geodetic (left-hand) system and the unknown parameters are computed than, secondly, transformed to the right-hand camera system.

In a first step the approximate coordinates are calculated because the observation equations used in the least squares adjustment are nonlinear. In a second step the redundant observations are adjusted with respect to the functional and the stochastic model. The rank defect of the normal equation system is eliminated by introducing a fixed geodetic datum.

3.2.1 Determine Approximate Values

As shown in fFigure 3 the approximate values for the unknown microphone positions are calculated with the observations from standpoint A only. The horizontal datum is parameterized by point A the horizontal x coordinate of point B that results the specified angle α from A to B.

Intersection

An expedient method in this case is the localization by an intersection of adjusted zenith and horizontal directions observed with a total station in conjunction with an adjusted base line and a prior information about the mutual microphone distance (Figure 3).

On each array arm only 3 out of 16 microphones are observed. Thus the orientation and the deflection of microphone arm can be estimated. The intermediate drilling holes are obtained by linear interpolation in a post adjustment process.

$$S_{A-Mic} = \frac{\sin \beta}{\sin(\alpha + \beta)} S_{A-B}$$

$$X_{Mic} = \cos(100^{(g)} - (\alpha + \delta)) S_{A-Mic}$$

$$Y_{mic} = \sin(100^{(g)} - (\alpha + \delta)) S_{A-Mic}$$

$$Z_{Mic} = \frac{S_{A-Mic}}{\tan(z_A^{Mic})}$$

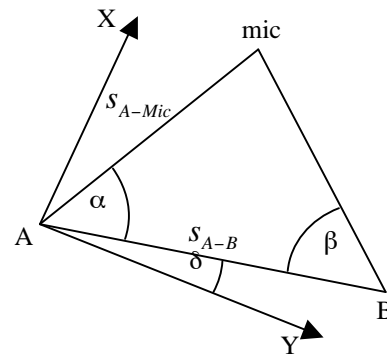


Figure 3 overview to calculate the approximativ values

3.2.2 Observation equations

The instrument reading for the **horizontal direction** is adjusted with respect to the unknown microphone coordinates, the standpoints and the zero horizontal direction ω .

$$r_A^{mic} + v_i = \arctan\left(\frac{y_{mic} - y_A}{x_{mic} - x_A}\right) - \omega_A \quad , \quad r_B^{mic} + v_{i+n} = \arctan\left(\frac{y_{mic} - y_B}{x_{mic} - x_B}\right) - \omega_B$$

$$r_A^B + v_{1+2n} = \arctan\left(\frac{y_B - y_A}{x_B - x_A}\right) - \omega_A \quad , \quad r_B^A + v_{2+2n} = \arctan\left(\frac{y_A - y_B}{x_A - x_B}\right) - \omega_B$$

Zenith angle from standpoint to microphone

$$\vartheta_A^{mic} + v_{i+2n+2} = \arctan\left(\frac{\sqrt{(y_{mic} - y_A)^2 + (x_{mic} - x_A)^2}}{z_{mic} - z_A}\right)$$

$$\vartheta_B^{mic} + v_{i+3n+2} = \arctan\left(\frac{\sqrt{(y_{mic} - y_B)^2 + (x_{mic} - x_B)^2}}{z_{mic} - z_B}\right)$$

Zenith angle from standpoint to standpoint

$$\vartheta_A^B + v_{1+4n+2} = \arctan\left(\frac{\sqrt{(y_B - y_A)^2 + (x_B - x_A)^2}}{z_B - z_A + h_A^B}\right)$$

$$\vartheta_B^A + v_{2+4n+2} = \arctan\left(\frac{\sqrt{(y_A - y_B)^2 + (x_A - x_B)^2}}{z_A - z_B - h_A^B}\right)$$

Slope distance between instrument points

$$s_A^B + v_{1+4n+4} = \sqrt{(x_B - x_A)^2 + (y_B - y_A)^2 + (z_B - z_A)^2}$$

$$s_B^A + v_{2+4n+4} = \sqrt{(x_A - x_B)^2 + (y_A - y_B)^2 + (z_A - z_B)^2}$$

Slope distances between drilling holes (a priori vendor information)

$$s_{mic}^{mic_i} + v_{i+4n+6} = \sqrt{(x_{mic_i} - x_{mic})^2 + (y_{mic_i} - y_{mic})^2 + (z_{mic_i} - z_{mic})^2}$$

3.2.3 Variance free datum

The three-dimensional left oriented measuring system has a rank defect of 5, since two rotational components are fixed due to the gravity (total station is leveled in both standpoints). The local instrument datum is a variance free base. Datum is given by

Translation: $x_A = y_A = z_A = 0.0 \text{ m} \pm 0.0 \text{ m}$
Rotation: $x_B = 0.1 \text{ m} \pm 0.0 \text{ m}$
Scale: a priori distance between drilled microphone holes $\pm 0.1 \text{ mm}$

3.2.4 Stochastic model

The stochastic model is given by the standard derivation of the horizontal and zenith direction with $\pm 0.3 \text{ mgon}$, the slope distance of the base with $\pm 1 \text{ mm}$ and slope distance between the microphones with $\pm 0.1 \text{ mm}$. Additionally the pointing error ($\pm 0.2 \text{ mm}$) is considered.

$$\sigma_{\text{point_rad}} = \frac{\sigma_{\text{point}}}{S_{ij}}$$

Horizontal and zenith directions with a given standard deviation of the unit weight $\sigma_0 = 1$ in the adjustment calculation are weighted

$$p_{\text{direction}} = \frac{\sigma_0^2}{\sigma_{\text{direction}}^2 + \left(\sigma_{\text{center_rad}} \frac{200}{\Pi}\right)^2}$$

Distant observations are weighted with

$$p_s = \frac{\sigma_0^2}{\sigma_s^2}$$

3.2.5 Least squares solution

The adjusted observations and unknowns are computed with the formulas for the parametric adjustment calculation like described in (Ghilani & Wolf, 2006) or (Niemeier, 2002).

Five star arrays were observed and adjusted (

Table 1). The assumptions for the stochastic and functional model are obviously true because the standard derivation of the unit weight after the adjustment is less than 1.

Furthermore a relationship between the distance to the array and the mean errors of the microphones is conspicuous. The closeness influenced the mean error of the microphone coordinates. To obtain the precise determination of the relative spatial positions of the microphones better than $\pm 0.5 \text{ mm}$, the maximal distance of a star array should not exceed 6m. To point out that no blunder influence the result the maximum normalized residuals NV for each star are shown.

number of the star array	1	2	3	4	5
distance to the star array [m]	4.36	4.37	4.73	5.48	6.14
baseline length [m]	4.21	4.21	4.59	4.59	4.59
mean of absolute corrections of the horizontal angles [mgon]	0.4	0.3	0.5	0.5	0.7
mean of absolute corrections of the zenith angles [mgon]	0.6	0.3	0.6	0.5	0.6
mean of the mean point errors of the local coordinates [mm]	0.22	0.13	0.3	0.45	0.51
maximum mean error of the local coordinates [mm]	0.26	0.15	0.41	0.51	0.59
max NV	1.1	0.7	2.1	2.8	2.1
$\hat{\sigma}_0$ after the adjustment	0.4	0.2	0.6	0.7	0.8

Table 1 solved adjustment results

3.3 Transformation into the target system

The results of the previous calculations are given in a local left oriented total station system that depends on the survey design. The next step is to transform the microphone coordinates from the left oriented total station system to the right orientated camera system. The datum of the target system is defined by approximate coordinates given by the microphone array vendor. As the solution of this transformation the residuals of the estimated geometric microphone position with respect to the designed theoretical spatial position of the microphones in the camera system is obtained.

3.3.1 Quaternion rotations

There are different possibilities to describe a rotation in the Euclidean space. Traditional Euler rotations suffer from the so called "gimbal lock" (Hanson, 2006), where a rotation maps one principle axis onto another, resulting in a loss of a degree of freedom. That's why good approximate values for the transformation parameter (three angles) are needed.

In order to avoid an intermediate calculation for the rotational approximation values and to guarantee convergence (quaternions are bi-linear) the rotation is parameterized with quaternions

$$q = q_0 + iq_1 + jq_2 + kq_3 = (q_0, q_1, q_2, q_3) = (q_0, \vec{q})$$

to which special operation rules are assigned (Hanson, 2006). For the rotation between the local and the demanded target system are used quaternions of unit length.

$$q \cdot q = q_0^2 + q_1^2 + q_2^2 + q_3^2 = q_0^2 + \vec{q} \cdot \vec{q} = 1$$

Quaternion represents a rotation by defining the plane of the rotation and the angle of the rotation. The plane is defined as normal to the quaternion vector n , and the angle is defined as α .

$$q_0 = \cos\left(\frac{\alpha}{2}\right); q_1 = n_x \cdot \sin\left(\frac{\alpha}{2}\right); q_2 = n_y \cdot \sin\left(\frac{\alpha}{2}\right); q_3 = n_z \cdot \sin\left(\frac{\alpha}{2}\right)$$

Like described in (Hanson, 2006) a rotation matrix can express with quaternion.

$$R = \begin{bmatrix} q_0^2 + q_1^2 - q_2^2 - q_3^2 & 2q_1q_2 - 2q_0q_3 & 2q_1q_3 - 2q_0q_2 \\ 2q_1q_2 + 2q_0q_3 & q_0^2 - q_1^2 + q_2^2 - q_3^2 & 2q_2q_3 - 2q_0q_1 \\ 2q_1q_3 - 2q_0q_2 & 2q_2q_3 + 2q_0q_1 & q_0^2 - q_1^2 - q_2^2 + q_3^2 \end{bmatrix}$$

With substituting in the diagonal elements with $q_0^2 + q_1^2 + q_2^2 + q_3^2 = 1$ it can be written like

$$R = \begin{bmatrix} 2q_0^2 + 2q_1^2 - 1 & 2q_1q_2 - 2q_0q_3 & 2q_1q_3 - 2q_0q_2 \\ 2q_1q_2 + 2q_0q_3 & 2q_0^2 + 2q_2^2 - 1 & 2q_2q_3 - 2q_0q_1 \\ 2q_1q_3 - 2q_0q_2 & 2q_2q_3 + 2q_0q_1 & 2q_0^2 + 2q_3^2 - 1 \end{bmatrix}$$

3.3.2 Estimation of the quaternion parameter

The presented approach models the designed coordinates X_{cam} in the camera system as observations. The rotation R is parameterized with the quaternion q_0, q_1, q_2, q_3 . The local coordinates X_{loc} are considered to be constant. The functional model is given with:

$$X_{cam} = R \cdot X_{loc} + T.$$

To separate the rotation R from the translation T a centroid reduction is performed before the rotation is estimated.

$$X_{cam_red} = R \cdot X_{loc_red}$$

Observation equations for the rotation are

$$x_{cam_red_1} + v_{x_1} = R_{11} \cdot x_{loc_red_1} + R_{12} \cdot y_{loc_red_1} + R_{13} \cdot z_{loc_red_1}$$

⋮

$$x_{cam_red_n} + v_{x_n} = R_{11} \cdot x_{loc_red_n} + R_{12} \cdot y_{loc_red_n} + R_{13} \cdot z_{loc_red_n}$$

$$y_{cam_red_1} + v_{y_1} = R_{21} \cdot x_{loc_red_1} + R_{22} \cdot y_{loc_red_1} + R_{23} \cdot z_{loc_red_1}$$

⋮

$$y_{cam_red_n} + v_{y_n} = R_{21} \cdot x_{loc_red_n} + R_{22} \cdot y_{loc_red_n} + R_{23} \cdot z_{loc_red_n}$$

$$z_{cam_red_1} + v_{z_1} = R_{31} \cdot x_{loc_red_1} + R_{32} \cdot y_{loc_red_1} + R_{33} \cdot z_{loc_red_1}$$

⋮

$$z_{cam_red_n} + v_{z_n} = R_{31} \cdot x_{loc_red_n} + R_{32} \cdot y_{loc_red_n} + R_{33} \cdot z_{loc_red_n}$$

The partial derivatives of the rotation matrix with respect to the quaternion parameter are given with.

$$\frac{\partial R}{\partial q_0} = \begin{bmatrix} 4q_0 & -2q_3 & 2q_2 \\ 2q_3 & 4q_0 & -2q_1 \\ -2q_2 & 2q_1 & 4q_0 \end{bmatrix}; \quad \frac{\partial R}{\partial q_1} = \begin{bmatrix} 4q_1 & 2q_2 & 2q_3 \\ 2q_2 & 0 & -2q_0 \\ 2q_3 & 2q_0 & 0 \end{bmatrix}$$

$$\frac{\partial R}{\partial q_2} = \begin{bmatrix} 0 & 2q_1 & 2q_0 \\ 2q_1 & 4q_2 & 2q_3 \\ -2q_0 & 2q_3 & 0 \end{bmatrix}; \quad \frac{\partial R}{\partial q_3} = \begin{bmatrix} 0 & -2q_0 & 2q_1 \\ 2q_0 & 0 & 2q_2 \\ 2q_1 & 2q_2 & 4q_3 \end{bmatrix}$$

Design matrix for the rotation into the target system.

$$A = \begin{bmatrix} \frac{\partial x_{cam_red_1}}{\partial q_0} & \frac{\partial x_{cam_red_1}}{\partial q_1} & \frac{\partial x_{cam_red_1}}{\partial q_2} & \frac{\partial x_{cam_red_1}}{\partial q_3} \\ \vdots & \vdots & \vdots & \vdots \\ \frac{\partial x_{cam_red_n}}{\partial q_0} & \frac{\partial x_{cam_red_n}}{\partial q_1} & \frac{\partial x_{cam_red_n}}{\partial q_2} & \frac{\partial x_{cam_red_n}}{\partial q_3} \\ \frac{\partial y_{cam_red_1}}{\partial q_0} & \frac{\partial y_{cam_red_1}}{\partial q_1} & \frac{\partial y_{cam_red_1}}{\partial q_2} & \frac{\partial y_{cam_red_1}}{\partial q_3} \\ \vdots & \vdots & \vdots & \vdots \\ \frac{\partial y_{cam_red_n}}{\partial q_0} & \frac{\partial y_{cam_red_n}}{\partial q_1} & \frac{\partial y_{cam_red_n}}{\partial q_2} & \frac{\partial y_{cam_red_n}}{\partial q_3} \\ \frac{\partial z_{cam_red_1}}{\partial q_0} & \frac{\partial z_{cam_red_1}}{\partial q_1} & \frac{\partial z_{cam_red_1}}{\partial q_2} & \frac{\partial z_{cam_red_1}}{\partial q_3} \\ \vdots & \vdots & \vdots & \vdots \\ \frac{\partial z_{cam_red_n}}{\partial q_0} & \frac{\partial z_{cam_red_n}}{\partial q_1} & \frac{\partial z_{cam_red_n}}{\partial q_2} & \frac{\partial z_{cam_red_n}}{\partial q_3} \end{bmatrix}$$

Because of the non invertible normal matrix $A^T P A$ we use the unit length condition for quaternions to solve the problem as parametric adjustment with conditions between the unknowns.

$$b = q_0^2 + q_1^2 + q_2^2 + q_3^2 - 1$$

$$\begin{bmatrix} x \\ k \end{bmatrix} = \begin{bmatrix} A^T P A & B \\ B^T & 0 \end{bmatrix}^{-1} \begin{bmatrix} A^T P l \\ w \end{bmatrix}$$

$$\text{with } B^T = \begin{bmatrix} \frac{\partial b}{\partial q_0} & \frac{\partial b}{\partial q_1} & \frac{\partial b}{\partial q_2} & \frac{\partial b}{\partial q_3} \end{bmatrix} = [2q_0 \quad 2q_1 \quad 2q_2 \quad 2q_3]$$

After an iteration process with guaranteed convergence we obtain the best estimated quaternion parameter to build the rotation matrix. Now we can compute the Translation parameter with the centroids in both coordinate systems and the rotation matrix.

$$T = \bar{x}_{cam_centroid} - R \cdot \bar{x}_{loc_centroid}$$

3.3.3 Result of the transformation

With the rotation and the translation matrix we obtain coordinated microphones in the camera system. In

Table 2 are carried together the maximum residuals for each star. It illustrates how different the geometric of each star is. Significant deflection of a microphone arm was not detected.

Star	max DX [mm]	max DY [mm]	max DZ [mm]
1	4.8	-6.3	1.9
2	6.4	-13.0	11.4
3	-9.3	7.8	-2.6
4	9.0	7.7	-6.2
5	-8.1	4.4	-5.9

Table 2 residuals of the star arrays

4. Outcome

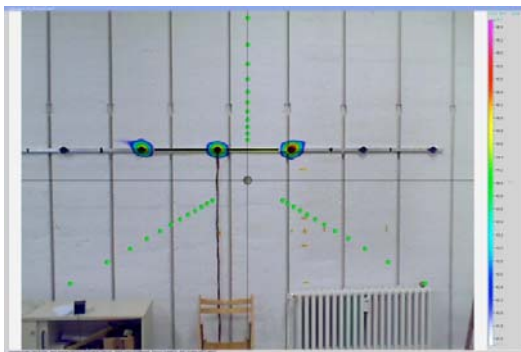


figure 4 and figure 5 illustrate the beamforming result of the time domain calculation as an acoustic image. Both images show a wall with tree active loudspeakers by an image contrast with 5 dB. The color scale on the right starts with transparent and deep blue with 40.3dB and increases over green until red and magenta 45.3 dB.

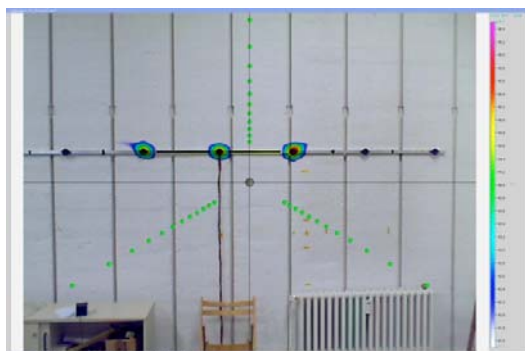


figure 4 shows the acoustic image before and figure 5 after the geometric calibration. The inexact time delay sets results a smudgy sound pressure map (

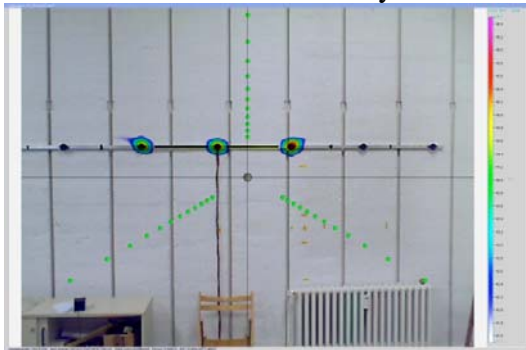


figure 4) so the sound sources cannot clearly localized. An intuitively understandable picture (figure 5) shows that tree loudspeaker in the middle were active and emit sound.

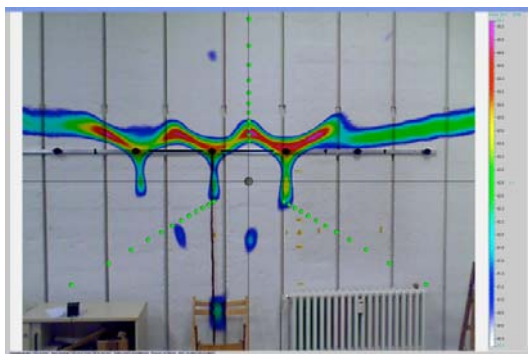


figure 4 acoustic image before calibration

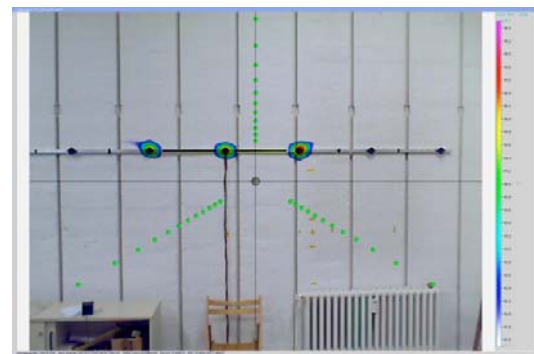


figure 5 acoustic image after calibration

REFERENCES

- Anderson, J. M., & Mikhail, E. M. (1998). *Surveying Theory and Practice*. Boston: McGraw-Hill.
- GFaI. (2008, 03). *acoustic-camera.com*. Retrieved 03 19, 2008, from <http://www.acoustic-camera.com/>
- Ghilani, C. D., & Wolf, P. R. (2006). *Adjustment Computations spatial data analysis*. Canada: John Wiley & Sons.
- Hanson, A. J. (2006). *Visualizing Quaternions*. San Francisco: Morgan Kaufmann.
- Jaeckel, O. (2006). Strengths and weaknesses of calculating beamforming in the time domain. Berlin Beamforming Conference (BeBeC).
- Niemeier, W. (2002). *Ausgleichsrechnung*. Berlin: de Gruyter .

BIOGRAPHICAL NOTES

Christian Manthe, born 1977. Graduated in 2006 as Dipl.-Ing in Surveying from Technische Universität Berlin. Since 2006 Assistant at the Department of Geodesy and Geoinformation Science, Technische Universität Berlin.

Andy Meyer, Graduated in 2002 as Dipl.-Ing in Surveying from Technische Universität Berlin. Since 2006 Assistant at the "Gesellschaft für angewandte Informatik e.V." (GFaI e.V. - Society for the promotion of Applied Computer Sciences)

Dr. Frank Gielsdorf, born 1960. Graduated in 1987 as Dipl.-Ing. in Surveying from Technical University of Dresden. Obtaining doctoral degree in 1997 from Technische Universität Berlin. 1995 Assistant Professor at the Department of Geodesy and Geoinformation, Technische Universität Berlin. Since 2007 Assistant at the technet GmbH

CONTACTS

Dipl.-Ing Christian Manthe
Technische Universität Berlin, Sekretariat H20
Strasse des 17. Juni 135
10623 Berlin
GERMANY
Tel. + 49 30 314 24147
Fax + 49 30 314 21119
email: christian.manthe@tu-berlin.de
Web site: www.survey.tu-berlin.de

Dipl.-Ing. Andy Meyer
Gfai
Rudower Chaussee 30
12489 Berlin
GERMANY
Tel. + 49 30 6395 1600
Fax + 49 30 6392 1602
email: meyer@gfai.de
Web site: www.gfai.de

Dr. Frank Gielsdorf
Techet GmbH
Massenstraße 14
10777 Berlin
GERMANY
Tel. + 49 30 215 4020
Fax. +49 30 215 4027
email: frank.gielsdorf@technet-gmbh.com
Web site: www.technet-gmbh.de

TS 6K – Traceability and Data Processing
Christian Manthe, Andy Meyer and Frank Gielsdorf
Geometric Calibration of acoustic camera Star48 array

15/15

Integrating Generations
FIG Working Week 2008
Stockholm, Sweden 14-19 June 2008